

C.P. No. 1319

C.P. No. 1319



LIBRARY  
ROYAL AIR FORCE  
ESTABLISHMENT  
BEDFORD.

PROCUREMENT EXECUTIVE, MINISTRY OF DEFENCE

AERONAUTICAL RESEARCH COUNCIL

*CURRENT PAPERS*

**A Theoretical and Experimental  
Investigation of the External-Flow,  
Jet-Augmented Flap**

*by*

*P. R. Ashill*

*Aerodynamics Dept., R.A.E., Bedford*

LONDON: HER MAJESTY'S STATIONERY OFFICE

1975

PRICE *f* 1-20 NET

A THEORETICAL AND EXPERIMENTAL INVESTIGATION OF THE  
EXTERNAL-FLOW, JET-AUGMENTED FLAP

by

P. R. Ashill

SUMMARY

There have been various attempts to devise a theoretical method for calculating the forces and moments acting on wings with external-flow, jet-augmented flaps. One of the simplest of these relies on the analogy between the internal-flow jet flap and the external-flow jet flap. To date, this method has been limited in application by its reliance on either measured or assumed values of the jet-deflection angle and the thrust-recovery factor, i.e. the factor that is applied to the momentum flux leaving the exit of the engine nacelle to allow for turning and spreading losses. This paper is concerned with a semi-empirical method for predicting these parameters. The method is based on an analysis of a series of tests performed on a wing, body and injector-powered nacelle under static conditions. The formulae derived from the analysis are combined with a theory, which is based on the jet-flap analogy, to provide estimates of the forces and moments acting on wings with external-flow, jet-augmented flaps in forward flight. Comparisons are made between this method and wind-tunnel data obtained from tests performed at the RAE and elsewhere.

*This paper was prepared for the AGARD Propulsion and Energetics Conference held at Schliersee, Germany, September 2973.*

CONTENTS

	<u>Page</u>
1 INTRODUCTION	3
2 CORRELATION OF STATIC-TEST DATA	4
2.1 Model, equipment and test technique	4
2.2 Method of correlation	5
3 METHODS FOR PREDICTING WIND-ON FORCES AND MOMENTS	10
3.1 Prediction of lift	10
3.2 Longitudinal force	16
3.3 Pitching moment	18
4 CONCLUSIONS	18
4.1 Static-turning performance	18
4.2 Forward flight	19
Appendix A Lift of an infinite, sheared jet-flap	21
Appendix B Determination of pitching moment	24
Table 1	29
Symbols	30
References	33
Illustrations	Figures 1-18
Detachable abstract cards	

1 INTRODUCTION

The external-flow jet-augmented flap is but one of several powered-lift configurations that are being considered for STOL transport aircraft and, in addition, for C/RTOL transport aircraft that are capable of approaching airfields at steep angles of descent. Two schemes have been proposed, one with the engines mounted on the upper surface of the wing and the other with the engines installed just beneath the wing. The present Report deals with the second scheme.

Numerous wind tunnel tests have been performed on models with external-flow jet flaps, mainly at NASA, and the basic trends of the overall forces with changes in thrust have been established. However, a basic understanding of the flow, including, for example, the way the efflux behaves after it impinges on the flap, has yet to be achieved. Fig.1 shows the effect of thrust on the overall forces for a typical engine-below-wing configuration and depicts the corresponding patterns displayed by the flow external to the jet. Although the changes in the forces seem to accord with intuition the effect of thrust on the flow is less straightforward.

Despite the absence of a complete understanding of the flow, attempts have been made to establish plausible theoretical models. The methods that have been proposed so far can be divided broadly into two groups. In the first group are methods<sup>1,2</sup> which rely on techniques that have been used, with some success, to predict the interference between propellor slipstreams and wings, whereas the second group comprises methods based on an analogy between the internal-flow jet flap and the external-flow jet flap<sup>2,3,4</sup>. A comparison between the two groups indicates that whilst the first group contains some representation of the influence of the efflux on the flow around the wing it makes no allowance for the inevitable flattening and spreading of the efflux following its impingement on the flap. In addition the two methods<sup>1,2</sup> of the first group have necessitated the writing of major computer programs. By contrast methods of the second group are simple in essence, being suitable for the routine evaluation of designs. On the other hand there are a number of detailed criticisms that can be levelled at them, the most serious of which is that these methods have, to date, employed measured or assumed values of the jet-deflection angle and the thrust-recovery factor, i.e. the factor that is applied to the gross thrust to allow for losses incurred in the turning and spreading of the efflux. Since these parameters are likely to depend on the position and orientation of the nacelle relative to the flap system this could restrict the range of configurations for which predictions could be made.

This paper is concerned therefore with a semi-empirical method for predicting the jet-deflection angle and the thrust-recovery factor. The method is based on an analysis of a series of tests performed on a wing, body and **injector-**powered nacelle under static conditions. These tests and the method used to correlate the results are described in section 2. In section 3 the formulae derived from the analysis of section 2 are combined with methods which use the jet-flap analogy, to provide estimates of the forces and moments acting on wings with external-flow, jet-augmented flaps in forward flight. These estimates are compared with wind-tunnel data obtained from tests performed at the RAE and NASA.

## 2 CORRELATION OF STATIC-TEST DATA

### 2.1 Model, equipment and test technique

The model, the equipment and the experiment have been described elsewhere<sup>5</sup> but for completeness a brief description is included here.

The model, a general arrangement of which is shown in Fig.2, comprised a half wing with a fuselage. Various tabbed flaps were fitted to the wing between the fuselage and 80% semi-span. The flap configurations tested are listed in Table 1; in this table and elsewhere in the paper the flap geometry is defined in terms of  $\theta_{F1}^0/\theta_{F2}^0$ , where  $\theta_{F1}$  is the flap deflection,  $\theta_{F2}$  the tab deflection relative to the flap, and suffixes (u) and (s) refer, respectively, to an unslotted or slotted tab. Fig.3 illustrates a typical flap configuration and shows the geometry of the leading-edge slat.

An injector-powered nacelle simulated a turbofan engine having a bypass ratio of the order of 3. During the tests the nacelle could be moved in the directions normal and parallel to the reference axis, i.e. the chord line of the basic wing. The position of the nacelle was defined by the coordinates  $(x_n, z_n)$ , where  $x$  is distance along the reference axis, in the downstream direction, from the leading edge of the basic wing at the **spanwise** station of the nacelle axis,  $z$  is vertical distance below the reference axis and suffix  $n$  refers to the position of the 'hot-jet' nozzle, which is varied within the rectangular area  $0.21 < z_n/c < 0.42$ ;  $0 < x_n/c < 0.4$ . In addition, the angle of the axis of the nacelle relative to the reference axis,  $\phi$ , could be varied within the range  $\pm 3^\circ$ , approximately,  $\phi$  being taken positive with the nacelle nosedown. Fig.3 shows the nacelle in a typical position relative to the wing.

Static tests were performed in a large room beneath the working section of the 13ft  $\times$  9ft wind tunnel at RAE Bedford, the efflux being directed out of the

building. Forces and moments were measured by a four-component, mechanical balance. For the majority of the static tests the thrust of the nacelle alone,  $T$ , was kept constant at 849 N (188 lbf) but a limited number of tests were performed at other thrusts in order to assess the effect of engine thrust on the static-turning performance of the configuration 40/30(s). It was found that the static-turning performance was insensitive to variations in thrust in the range 226 N (50 lbf) to 903 N (200 lbf).

Wind-tunnel tests, which will be referred to in connexion with the comparison between the wind-on theory and experiment, were performed with the model in the 13ft  $\times$  9ft wind tunnel at a wind speed of 37 m/s (120 ft/s).

## 2.2 Method of correlation

A method was given in Ref.5 for correlating the results of static-turning tests. This method was developed specifically for the case of a jet-pitch angle  $\phi_e = 0$ . However, a purely empirical technique was presented<sup>5</sup> for reducing the data to equivalent values for zero jet-pitch angle. The data obtained for the configurations of Table 1 support the use of this technique for values of the jet-pitch angle between  $-2^\circ$  and  $4^\circ$ . On the other hand, measurements made at Dornier AG<sup>6</sup> of the static-turning performance of an external-flow, jet-flap configuration with a jet-pitch angle of  $20^\circ$  indicate that the method of Ref.5 is unsuitable for values of the jet-pitch angle that are in excess of  $10^\circ$ . Since nacelle-pitch angles that are greater than  $4^\circ$  seem unlikely in practice this may not appear to be a significant limitation. There have, however, been suggestions<sup>7,8</sup> that for aircraft with external-flow jet flaps the nacelles might be equipped with efflux deflectors, and it is conceivable that by careful design such deflectors could increase the jet-pitch angle by as much as  $10^\circ$ . Accordingly, the analysis of Ref.5 is extended here in a fairly simple way to include **nonzero**, jet-pitch angles. The model of the jet flow employed in the extended analysis is shown in Fig.4. It will be seen there that the efflux is divided into two regions; the region of the efflux that is captured by the flap (i.e. the part of the cross-section of the undistorted efflux that projects onto the flap) is assumed to leave the trailing edge of the flap at an angle  $\theta_c$  to the reference axis. It is anticipated that in practice this angle will be approximately equal to the overall flap angle  $\theta_F$ . The remaining part of the efflux is supposed to be unaffected by the presence of the flap. Thus with the suffixes c and J referring respectively to the captured part of the jet and the jet as a whole we have from momentum considerations

$$\left. \begin{aligned} \eta_c M_c \sin(\theta_c + \phi_e) &= \eta_J M_J \sin(\theta_J + \phi_e) \\ M_J = M_c + \eta_c M_c \cos(\theta_c + \phi_e) &= \eta_J M_J \cos(\theta_J + \phi_e) \end{aligned} \right\}, \quad (1)$$

where  $M$  is momentum flux and  $\eta$  is the thrust-recovery factor.

With the aid of simple **geometrical** arguments and by assuming that the density and velocity are uniform within the jet, it is **found**<sup>5</sup> that, for a round jet of diameter  $D_J$ ,

$$M_c/M_J = \left[ \lambda(1 - \lambda^2) + \pi/2 + \sin^{-1} \lambda \right] / \pi, \quad (2)$$

where 
$$\lambda = 2z_T/D_J \quad (3)$$

and  $z_T$  is the minimum distance between the axis of the jet and the trailing edge of the flap,  $z_T$  being taken positive when the flap trailing edge is below the axis of the jet. The further assumption was made in Ref.5 that the diameter of the jet is equal to the diameter of the bypass nozzle. This was justified for the configurations examined in Ref.5 by noting that the part of the efflux that lay upstream of the flap belonged to the initial region of the jet and consequently spread slowly. This approach does, however, have the fault that it does not allow for the slight spread of the jet in this region. Accordingly the analysis has been modified to allow for jet spread. This is achieved, firstly by assuming that the virtual origin of the jet is situated at the exit of the bypass nozzle, secondly by taking the diameter of the jet at the origin to be the diameter corresponding to the total nozzle area, and by assuming that the sides of the jet spread with an angle of  $5^\circ$  to the jet axis. This is the angle of the 10% velocity line in the initial region of a round jet emerging into still air<sup>9</sup>.

By using this simple theoretical framework it has been **possible**<sup>5</sup> to deduce values of the thrust-recovery factor  $\eta_c$  and the deflection angle  $\theta_c$  associated with the captured part of the efflux. In order to analyse these data, consideration is given to an extension of a correlation presented in Ref.5 for the case of zero jet-pitch angle. This correlation is based on the physically plausible assumption that the thrust-recovery factor of the captured part of the flow,  $\eta_c$ , depends mainly on the total angle turned by the captured flow,  $(\theta_c + \phi_e)$ . Fig.5 shows the result of attempting to produce a correlation

of this form for the present model and for **models** tested by Dornier AG<sup>6</sup> and NASA<sup>7,8,10</sup>. These configurations share the property that the lowest slot of the flap was no more than one jet diameter above the axis of the jet. It is seen that the correlation is fairly satisfactory and is approximated quite well by the **empirical** expression

$$\eta_c = \cos^2 (\theta_c + \phi_e) + 0.636 \sin^2 (\theta_c + \phi_e) . \quad (4)$$

Also shown for comparison is the curve derived from a simplified model of the frictionless flow of a jet impinging on a flap which is of flat-plate section and deflected through an angle  $\theta_c$ . In this model the jet separates smoothly from both the leading edge and the trailing edge of the flap, the jet sheet being considered thin enough for the streamlines in each streamwise section to be supposed parallel to the flap at separation. In this case it is readily found that

$$\eta_c = \cos (\theta_c + \phi_e) . \quad (5)$$

The corresponding curve illustrates the importance of ensuring that the jet is able to sustain itself around the nose or noses of the flap system, particularly for turning angles in excess of  $50^\circ$  where the values of  $\eta_c$  deduced from equation (4) are significantly larger than those obtained from equation (5).

Having established what seems to be a reasonable basis for estimating the thrust-recovery factor of suitably designed nacelle-flap configurations we now consider a means of correlating the angle turned by the captured part of the flow. Fig.6 shows a plot of

$$\kappa = \sin (\theta_c + \phi_e) / \sin (\theta_F + \phi_e) \quad (6)$$

against the ratio of the momentum flux captured by the flap to the total momentum flux of the jet prior to impingement,  $M_c/M_J$ , for the two flap configurations 40/0(u) and 40/30(s). An interesting feature of these plots is that  $\kappa$  appears to be sensibly constant for values of  $M_c/M_J$  less than 0.4. Furthermore, it seems that an acceptable approximation to  $\kappa$  in this region can be obtained by assuming that

$$\theta_c = \theta_{F_u} ,$$

leading to

$$\kappa = \sin(\theta_{F_U} + \phi_e) / \sin(\theta_F + \phi_e), \quad 0 \leq M_c/M_J \leq 0.4, \quad \dots \dots (7)$$

where  $\theta_{F_U}$  is the angle in a chordwise plane between a line tangential to the upper boundary of the flap at the flap trailing edge and the reference axis. This assumption might be justified on the basis that the majority of the captured flow passes through the flap slot or slots and is turned by the Coanda effect so that it leaves the flap trailing edge in a direction that is tangential to the flap upper surface. However, whilst this assumption might be justified for small values of the parameter  $M_c/M_J$ , Fig.6 shows that it is not satisfactory when the majority of the jet is captured. Fortunately, the parameter  $\kappa$  can be represented quite well in the interval  $0.4 < M_c/M_J \leq 1$  by the simple, linear relationship

$$\kappa = \kappa^* + C(1 - M_c/M_J), \quad (8)$$

where  $\kappa^*$  is the value of the parameter  $\kappa$  when the jet is fully captured and  $C$  is given by

$$C = \frac{1}{0.6} \left[ \frac{\sin(\theta_c + \phi_e)}{\sin(\theta_F + \phi_e)} - \kappa^* \right]. \quad (9)$$

As indicated in Fig.6 the parameter  $\kappa^*$  depends on the total angle turned by the captured flow. This dependence is confirmed by Fig.7 which shows a plot of  $\kappa^*$  against  $\sin(\theta_c + \phi_e)$ , the points shown being deduced from two independent sources<sup>6,10</sup> as well as from the present tests. Evidently the parameter  $\kappa^*$ , which may be regarded as a measure of the effectiveness of the flap as a device for turning a fully-captured jet, increases as the turning angle becomes larger, apparently reaching a value close to unity when the jet is turned through a right angle. The most likely explanation for this trend seems to be that as the flap angle (and hence turning angle) increases the jet becomes increasingly flattened after impingement with the result that the jet is more able to follow the flap contour. Against this must be set the fact that, with the increased tendency for the jet to spread laterally across the flap, the thrust-recovery factor decreases with increasing turning angle as indicated in Fig.5.

A suitable mean curve through the experimental points in Fig.7 can be defined by the relationship

$$\kappa^* = 0.6 + 0.4 \sin (\theta_c + \phi_e) \quad (10)$$

To two significant figures this expression degenerates to the result given by the linear, or small-angle, theory for a wing spanning a round jet<sup>11</sup> when the turning angle is zero. However, as shown in Fig.7, equation (10) represents a significant improvement over the linear theory which of course makes no allowance for the distortion of the jet after impingement on the flap.

Equation (10) is an implicit equation for the turning angle of a **fully-captured** efflux; this expression can be rearranged, however, to yield the explicit result

$$\kappa^* = 0.6_I (1 - 0.4 \sin (\theta_F + \phi_e)) \quad (11)$$

Our final remarks in this section concern the determination of the overall thrust-recovery factor  $\eta_J$  and the jet-deflection angle  $\theta_J$ . Referring to equation (1) we find that it is possible to write

$$\eta_J = \left[ (\eta_c M_c)^2 + (M_J - M_c)^2 + 2\eta_c M_c (M_J - M_c) \cos (\theta_c + \phi_e) \right]^{1/2} / M_J \quad (12)$$

$$\tan (\theta_J + \phi_e) = \frac{\eta_c M_c \sin (\theta_c + \phi_e)}{M_J - M_c + \eta_c M_c \cos (\theta_c + \phi_e)} \quad (13)$$

By using these expressions in combination with equations (4), (7), (9) and (11) it is possible to determine the two static-turning parameters, given:

- (a) overall flap angle;
- (b) jet-pitch angle;
- (c) diameter of the bypass nozzle;
- (d) position of the nacelle in relation to the flap.

In the following section we describe how these results may be combined with methods based on the jet-flap analogy to yield forces and **moments** acting on wings with external-flow jet flaps at forward speed.

3 METHODS FOR PREDICTING WIND-ON FORCES AND MOMENTS3.1 Prediction of lift

**Perry**, in his analysis <sup>3</sup> of the lift of wings with external-flow jet flaps, used a semi-empirical formula that was suggested by Williams, Butler and Wood <sup>12</sup>. This formula, which is based on the theoretical treatment of unswept jet flaps of high aspect ratio by Maskell and Spence <sup>13</sup>, was intended to cater for **part-span** flaps. A similar approach is used in the present paper to derive an expression including the effects of sweep and the increase in **planform** area implied by the use of extending-chord flaps.

To deal with the influence of sweep, consideration is given firstly to the case of an infinite sheared wing of sweep  $\psi$  with a full-span, jet-augmented flap of constant sectional-momentum coefficient  $C'_\mu = J/\frac{1}{2}\rho U_\infty^2 c_e$ , where  $J$  is the local jet momentum at the trailing edge and  $c_e$  is the (extended) chord of the wing. In Appendix A it is shown that according to the linearized theory the sectional lift coefficient of such a wing is given by

$$C_L^{(s)}(C'_\mu) = \cos \psi C_L^{(2)}(C'_\mu \sec \psi) ,$$

where  $C_L^{(2)}(C'_\mu)$  is the sectional lift coefficient of the corresponding **two-dimensional** wing at the same sectional momentum coefficient, both lift coefficients being based on the extended chord  $c_e$ .

The effect of finite aspect ratio is included by using the method of Maskell and Spence <sup>13</sup> and by assuming that the sectional properties of a swept wing of large aspect ratio can be approximated adequately by those of the sheared region. This approximation probably fails in both the root and tip regions of the wing. However, it is known <sup>14</sup> that in the case of an 'unblown' wing the sectional lift increases in the root region by an amount almost equal to the amount it decreases at the tip. Therefore the sheared-wing approximation is likely to be adequate for the determination of the overall lift coefficient,  $C_L$ . Consequently it is found that

$$C_L = sFC_L^{(s)} , \quad (14)$$

where  $s = S_e/S$  is a factor allowing for the increase in the **planform** area from that of the basic wing with flaps retracted,  $S$ , to that of the wing with the flaps deployed  $S_e$ . The aspect-ratio factor

$$F = \frac{A + (2/\pi)C_{\mu}}{A + s \left\{ (2/\pi) \left( \partial C_L^{(s)} / \partial \alpha \right) - 2(1 + \sigma) \right\}}, \quad (15)$$

where  $A$  is the aspect ratio of the basic wing;

$C_{\mu}$  is the overall momentum coefficient based on the gross **planform** area of the basic wing;

$\sigma$  is a quantity which, for a high-aspect-ratio wing of moderate or small sweep and small  $C_{\mu}$ , is small and positive.

In the present calculations the parameter  $\sigma$  has been placed equal to zero. Note that with this approximation, and in the limit as the sectional momentum coefficient goes to zero, equation (14), with equation (15), is in agreement with equation (106) of Thwaites<sup>14</sup> (p.327) for an unblown, swept wing of large aspect ratio and with an elliptic distribution of circulation across the span.

By following Williams, Butler and Wood<sup>12</sup> the effects of flap span and wing thickness are accommodated in a semi-empirical manner by writing

$$C_L = sF \left[ \left\{ 1 + (t/c_e) \sec \psi \right\} \left( \mu_1 \theta \left( \partial C_L^{(s)} / \partial \theta \right) + \mu_2 \alpha \left( \partial C_L^{(s)} / \partial \alpha \right) \right) \right] - (t/c_e) \sec(\psi) C_{\mu} (\theta + \alpha), \quad (16)$$

where  $\theta$  is the effective flap angle,

$\alpha$  the incidence,

$$\mu_1 = \frac{S'}{S_e},$$

$$\mu_2 = \frac{S' \left( \partial C_L^{(s)} / \partial \alpha \right) + (S_e - S') \left( \partial C_L^{(s)} / \partial \alpha \right)_{C'_{\mu}=0}}{S_e \left( \partial C_L^{(s)} / \partial \alpha \right)},$$

and  $S'$  is the **planform** area of the wing corresponding to the **spanwise** extent of the flap. This area may or may not include the straightforward extrapolation of the wing area into the fuselage depending on the nature of the wing-fuselage junction, a matter that will be taken up again later. In the evaluation of the sectional derivatives the mean sectional-momentum coefficient  $C'_{\mu} = C_{\mu} S/S'$  is employed. The effect of thickness is included by applying the factor  $\{1 + (t/c_e) \sec \psi\}$  to the 'circulation' component of the lift, i.e. the overall lift minus the jet-reaction component of lift. This factor has its origin in

Perry replaced the effective flap angle  $\theta$  by the jet-deflection angle  $\theta_J$  and based his estimate of the overall momentum coefficient on the gross thrust factored by the thrust-recovery factor  $\eta_J$ . This approach would seem to be best suited to configurations for which the majority of the efflux is captured by the flap, and Perry confined his analysis to this type of configuration. Equally it is probable that Perry's approach is not justified when the major part of the efflux passes beneath the flap. This may be demonstrated by reference to equation (13) which shows that, for the case of zero jet-pitch angle, the jet-deflection angle is zero when no part of the efflux is captured by the flap, regardless of flap angle. However a null value for the effective flap angle is unlikely to be representative for a wing with flaps deflected, in general, even if the efflux passes completely beneath the flap. Support for this view is also provided by **Fig.8a** and b. These figures show a comparison between equation (16), evaluated by using Perry's method, and the lift coefficients obtained from wind-tunnel tests on the present model with the flap configurations 40/0(u) and 40/30(s), respectively. The comparison is made for a gross-thrust coefficient,  $C_{TG} = M_J / \frac{1}{2} \rho U_\infty^2 S$  of 0.82. The agreement between theory and experiment is particularly poor for the lowest nacelle position. Indeed for the configuration 40/0(u),  $z_n/c = 0.406$  the theory yields virtually no lift at zero incidence because the jet-deflection angle is approximately zero in that case. In an attempt to meet this criticism consideration has been given to an alternative theory that is more in keeping with the spirit of the analysis of section 2. Use is made of the implicit assumption of the method of section 2 that only the captured part of the efflux spreads to form a jet sheet downstream of the trailing edge of the flap. It seems reasonable to suppose that the remainder of the efflux does not influence the circulation around the wing, although its contribution to the jet-reaction lift is retained. Hence the momentum coefficients  $C_\mu$  and  $C'_\mu$  in equation (16) are replaced by

$$C_{\mu_c} = M_c / \frac{1}{2} \rho U_\infty^2 S, \quad C'_{\mu_c} = M_c / \frac{1}{2} \rho U_\infty^2 S'.$$

In addition it is noted that over the majority of the flap span the captured part of the efflux is likely to be 'thin' when it leaves the trailing edge of the flap. Therefore for an **inviscid** flow the effective flap angle may be supposed equal to the overall flap angle  $\theta_F$ . As may be inferred from Fig.6 this implies an error in the jet-reaction component of the lift. However this error is generally small and, as will be seen later, is removed without difficulty.

**Fig.8a** and b show the lift-incidence curves predicted by this alternative method for the RAE model. In these calculations, as in the calculations performed by using Perry's approach,  $\psi$  was taken to be the sweep of the **mid-chord** line of the basic wing. Furthermore since the flap did not abut the fuselage (**Fig.2**), the area  $S'$  was taken to be the area of the wing corresponding to the span of the exposed flap. In the evaluation of the increment in sectional lift due to flap deflection, allowance was made for the fact that for some of the configurations examined the streamwise section of the flap comprised more than one element. With such configurations the linear principle of superposition was exploited to construct the solution for the lift increment.

It is seen in **Fig.8a** and b that, generally, the alternative method overestimates the lift, the discrepancy being most obvious for the lowest nacelle position. This can be mainly attributed to three factors. First, it is well known that the linearized theory, on which the present method is based, overestimates the lift increment, due to flap deflection, of an aerofoil with an unblown flap even in potential flow. Second, the displacement effect of the boundary layer on the flap upper surface tends to impair the lifting **effective-**ness of the flap<sup>15</sup>, although this tendency would be expected to decrease as the momentum of the part of the efflux passing through the slots increases. Third, the linearized theory necessarily overestimates the jet-reaction lift since, for example, it replaces  $\sin(\theta_c + \alpha)$  by  $\theta_c + \alpha$ .

As regards the first effect it is interesting to observe that according to the alternative theory the increment in circulation lift, due to the jet sheet, is small compared with the overall lift for typical flap-nacelle configurations. This is illustrated in **Fig.9** for one such configuration, and it is seen that the incremental circulation lift is approximately 11% of the overall lift for values of  $C_{\mu}$  between 2 and 6. Thus for the purpose of correcting the circulation component of lift for non-linearities associated with flap deflection it is permissible to refer to the theory for wings with unblown flaps. However even without blowing there are, at present, no known exact solutions for three-dimensional wings in potential flow. In the absence of such solutions use will be made of an exact solution given by Hay and Eggington<sup>16</sup> for the two-dimensional, potential flow about a flat-plate aerofoil with a plain flap. **Fig.10**, which is based on their results, shows a plot of

$$H(\theta, \alpha) = \frac{\Delta C_{L_{\theta}}^{(s)}}{\left(\Delta C_{L_{\theta}}^{(s)}\right)_{\theta}}$$

against the effective flap angle  $\theta$  for the case of an aerofoil with a flap chord  $c_f = 0.3 c_e$ , where  $\Delta C_{L\theta}^{(s)}$  is the increment in sectional lift coefficient due to flap deflection, suffix  $\ell$  referring to the linearised theory. Thus the corrected increment in circulation lift due to flap deflection may be written as:

$$\Delta C_{L\theta}^{(\Gamma)} = H(\theta_F, \alpha) \left( \Delta C_{L\theta}^{(\Gamma)} \right)_\ell, \quad (17)$$

where superscript (I') refers to the circulation component of lift.

If the parameter H properly accounts for the non-linearities in the incremental circulation lift due to flap deflection it is reasonable to expect that any remaining discrepancies between the incremental circulation lifts as predicted and as measured can be attributed to the second of the effects outlined above, namely the displacement effect of the flap boundary layer. Consequently it might be argued, by analogy with the results of numerous **flap-blowing studies**<sup>14</sup>, that the parameter

$$G = \left( \Delta C_{L\theta}^{(\Gamma)} \right)_M / \Delta C_{L\theta}^{(\Gamma)} \quad (18)$$

will correlate against  $C_{\mu_c}^I$ , for a given flap configuration and at a given Reynolds number, regardless of nacelle position and orientation. Here suffix M refers to the measured value of the incremental circulation lift. Note that the sectional momentum coefficient  $C_{\mu_c}^I$  is considered to be more appropriate than the coefficient  $C_{\mu}^I$  since it seems probable that only the captured part of the efflux will affect the boundary layer on the flap upper surface.

The result of attempting to correlate the parameter G against the sectional momentum coefficient of the captured flow is shown in Fig.11 for various flap-nacelle configurations and for **incidences** ranging from  $0^\circ$  to an incidence  $2^\circ$  below the stall. In the determination of the parameter G for the configurations of **Refs.10** and 17 it was noted that both of these configurations had wings that were mounted high on the fuselage and with flaps that appeared to abut the fuselage. Therefore it was considered appropriate in these cases to include in the area S' the area obtained by extrapolating the wing **planform** into the fuselage.

Fig.11 provides some support for the contention made above regarding the correlation. The full line shown may be considered, in the absence of a **more** basic study, as a reasonable working approximation for values of  $C'_{\mu c}$  between 0.5 and 3, regardless of the type of configuration and the Reynolds number. In the interval  $0 < C'_{\mu c} < 0.5$  there are significant differences between the values of the parameter G for the various configurations, an indication of the differing degrees of effectiveness of the basic, unblown flaps as devices for controlling the boundary layer on the flap. It seems probable therefore that in this interval the parameter G is sensitive to Reynolds number, and it is suggested that this parameter may be obtained by fairing the full line into the value for zero momentum coefficient. This procedure could prove useful if the lifting properties of the unblown flap have already been established. Fig.11 illustrates the process for the two configurations of the present model 40/0(u) and 40/30(s).

It only remains to incorporate in the alternative method the above corrections for the errors in the jet-reaction component of lift due both to the neglect of non-linear terms and to the use of the assumption that the effective flap angle is equal to the overall flap angle. When these corrections are included and use is made of equations (16), (17) and (18) the final expression for the lift coefficient becomes:

$$C_L = G(C'_{\mu c})H(\theta_F, \alpha) \left( \Delta C_{L\theta}^{(\Gamma)} \right)_\ell + \left( \Delta C_{L\alpha}^{(\Gamma)} \right)_\ell + \eta_J C_{T_G} \sin(\theta_J + \alpha), \quad (19)$$

with

$$\left( \Delta C_{L\theta}^{(\Gamma)} \right)_\ell = sF \left\{ 1 + (t/c_e) \sec \psi \right\} \mu_1 \theta_F \left( \partial C_L^{(s)} / \partial \theta \right) - \left\{ 1 + (t/c_e) \sec \psi \right\} C_{\mu c} \theta_F, \quad (20)$$

and

$$\left( \Delta C_{L\alpha}^{(\Gamma)} \right)_\ell = sF \left\{ 1 + (t/c_e) \sec \psi \right\} \mu_2 \alpha \left( \partial C_L^{(s)} / \partial \alpha \right) - \left\{ 1 + (t/c_e) \sec \psi \right\} C_{\mu c} \alpha. \quad (21)$$

Note that the increment in circulation lift due to incidence, at zero flap deflection, which in the linearised theory is given by the term  $\left( \Delta C_{L\alpha}^{(\Gamma)} \right)_\ell$ , has not been corrected for non-linear effects. Allowance could be made by replacing  $\alpha$  in equation (21) with  $\sin \alpha$ , as in **the** classical theory for the lift on a two-dimensional, flat plate. However it seems doubtful whether this correction results in a significant improvement in accuracy, at least in the range of **incidences** of interest.

It may seem strange that the lift on a wing with an external-flow jet flap can be predicted with reasonable accuracy by a theory that is based on a method developed for a wing with a uniform distribution of momentum coefficient across the span. Results from **tests**<sup>6</sup> have shown that the distribution of jet momentum across the span of a wing with an external-flow jet flap is very uneven, with the major part of the jet momentum being confined to a limited part of the span. However it will be recalled from Fig.9 that according to the uncorrected version of the alternative theory the increment in circulation lift, due to the induction effect of the jet sheet on the flow around the wing, is small compared with the overall lift. Hence it is considered that in general the errors in the present method, due to the failure to represent the precise distribution of jet momentum across the span, are not likely to be serious.

**Fig.12a** and **b** illustrate how the present method, equation (19), might be used to predict the effect of the height of the nacelle centre-line on lift for the configurations 40/0(u) and 40/30(s). It is seen that with the function  $G(C'_{\mu_c})$  interpolated in the manner outlined above equation (19) follows the trends of lift with engine height with reasonable accuracy. Also shown are the predictions of Perry's version of the jet-flap analogy for the case  $\phi_e = 4.4^\circ$ , the lift given by equation (16) being factored by Perry's empirical functions  $f_1$  and  $f_2$ . As foreshadowed by **Fig.8a** and **b**, Perry's method severely underestimates the lift for the low nacelle positions, and it would seem that Perry's **method** cannot be used with confidence when the majority of the efflux passes beneath the flap.

A comparison between the present method, Perry's method and the test data of Ref.17 is shown in **Fig.13a** and **b** for the two engine positions 1 and 4, the lift being plotted against incidence. These figures merely confirm that both methods give satisfactory predictions of lift when the major part of the efflux is captured by the flap.

### 3.2 Longitudinal force

Perry' has provided a useful review of the methods available for predicting the longitudinal force of wings with jet flaps. However, he found that none of these methods was suitable for external-flow jet flaps. As an alternative he suggested regarding the flap as a simple thrust-deflector; that is to say he ignored the induction effect of the jet sheet on the flow around the wing. With this approximation the expression for the longitudinal-force coefficient becomes

$$C_A = C_\mu \cos(\theta_J + \alpha) - \frac{(C_L^{(\Gamma)})^2}{\pi A} - C_{D_0} - C_{D_M} \quad (22)$$

where  $C_{D_0}$  is the boundary-layer drag coefficient associated with the flow external to the jet and  $C_{D_M}$  is the coefficient of intake momentum drag, all coefficients in this expression being based on the gross **planform** area of the basic wing. This approach may be reconciled with classical jet-flap theory if the span of the jet sheet at the trailing edge of the flap is small compared with the mean (extended) chord of the wing. It is therefore relevant to recall that the indications are that the jet sheet associated with each of the nacelles of a typical, external-flow jet flap is of limited **spanwise** extent.

In the calculation of the longitudinal force coefficient by equation (22) the momentum coefficient,  $C_\mu = \eta_J C_{TG}$ , and the jet-deflection angle were obtained from the results of section 2. The circulation component of lift was derived by means of the alternative method of section 3.1, i.e. with corrections for non-linear effects and boundary-layer displacement. The determination of the boundary-layer drag  $C_{D_0}$  poses a major problem owing to the fact that an unquantified proportion of the wing area is submerged in the efflux or effluxes and therefore the 'drag area' associated with the external flow is unknown. In view of this **uncertainty, estimates** were made of the boundary-layer drag coefficient  $C_{D_0}$  by assuming that the flap is unblown, and the value used is quoted where appropriate. The intake-momentum drag was evaluated by making use of an inviscid, one-dimensional theory<sup>18</sup> for injector units, suitably corrected for viscous losses due to, for example, the boundary layers on the sidewalls of the nozzles.

**Fig.14a** and **b** illustrate a comparison between results from the **thrust-deflector** method and data taken from tests on the present model. The longitudinal force is plotted against lift for the flap configurations **40/0(u)** and **40/30(s)** and for various nacelle heights; it is seen that the method predicts both the effect of lift and the influence of nacelle height on the longitudinal force reasonably well.

A comparison between the thrust-deflector method and test data of Ref.17 is shown in **Fig.15a** and **b** where longitudinal force is plotted against lift for engine position 1, two flap angles and three gross-thrust coefficients. Again the predictions of the thrust-deflector theory are found to be satisfactory.

### 3.3 Pitching moment

A method for determining the pitching moment of a wing with an **external-flow jet flap**, which follows essentially the method of section 3.1 for determining the lift, is presented in Appendix B. When comparing results from this method with data for wing-body configurations the allowance made for the fuselage is essentially the same as that made in connexion with the estimation of lift. For example, in the case of the RAE model, the flaps are assumed to have a cut-out at the root, the span of which is equal to the fuselage diameter.

The theoretical trim curves are shown in Fig.16a and b for the RAE model with the flap configurations 40/0(u) and 40/30(s). The agreement between these estimates and the corresponding data for the three nacelle heights is only moderate but the effect on the pitching moment of a change in engine vertical position is reasonably well represented. It is thought that the reason for the lack of good agreement is that the effect of the fuselage on the pitching moment is not adequately represented by the theory. Whilst the present theory may simulate the junction effect properly, it does not include the pitching moment resulting from the lift developed on the **forebody** and the afterbody when the local angle of incidence is **nonzero**. Simple calculations of this body effect, which are based on slender-body theory<sup>14</sup> and which allow for the fact that the trailing vortices influence the local angle of incidence of the afterbody, yield corrections to the pitching **moment** that are approximately equal to the **discrepancies** between the curves and the test data in Fig.16a and b.

Fig.17a and b show a comparison between the present theory and the test data of Ref.17 for the two engine positions 1 and 4 with the flap angle  $\theta_F \simeq 60^\circ$  in both cases. The theory is seen to represent the effect of gross thrust on the trim curves reasonably well.

## 4 CONCLUSIONS

The following conclusions have been reached in this Report.

### 4.1 Static-turning performance

By using a method, based on simple momentum relationships, it has been possible to correlate experimental results for the thrust-recovery factor and the jet-deflection angle for various flap-nacelle configurations under static conditions.

## 4.2 Forward flight

### (a) Lift

Perry's<sup>3</sup> version of the jet-flap analogy is found to be restricted to configurations for which the majority of the efflux is captured by the flap. To overcome this possible drawback an alternative method has been devised. This approach appears to answer the requirement for a simple method that is capable of providing reasonable predictions of the lift of a wide variety of flap-nacelle configurations. Further wind-tunnel tests are required to assess the possible limitations of the method.

### (b) Longitudinal force

The longitudinal force acting on various configurations has been estimated by using Perry's thrust-deflector hypothesis. The predictions of this method regarding the effects of nacelle vertical position, thrust and incidence appear to be satisfactory.

### (c) Pitching moment

Whilst the absolute values of pitching moment are not predicted with good accuracy by the theory of Appendix B it represents fairly well the trends associated with changes in nacelle vertical position and gross thrust.

Appendix A

LIFT OF AN INFINITE, SHEARED JET-FLAP

The coordinate systems and notation used in the following discussion of the lift of an infinite sheared wing with a jet flap, which are illustrated in **Fig.18**, are basically similar to that used by Thwaites<sup>14</sup> in the case of the unblown, sheared wing.

According to Maskell and Spence<sup>13</sup> the pressure difference across a thin jet sheet may be written as

$$\Delta p = \left( \kappa_1 V_1^2 + \kappa_2 V_2^2 \right) \rho_J \delta_J \quad , \quad (\text{A-1})$$

where  $\kappa_1, \kappa_2$  are the principal curvatures of the sheet,  $V_1, V_2$  are the velocity components along the lines of curvature, and  $\delta_J$  is jet thickness. For an infinite, sheared wing it seems reasonable to anticipate that the cross-sectional shape of the jet in each of the planes  $Y = \text{constant}$  is independent of position along the generators. In other words it is asserted that the jet has zero curvature in planes  $X = \text{constant}$ . Consequently, with  $V_J$  the velocity of the jet in the free-stream direction, it is possible to write

$$\kappa_1 = \kappa_X \quad , \quad V_1 = V_J \cos \psi \quad , \quad \kappa_2 = 0 \quad ,$$

with  $\kappa_X$  the curvature of the jet sheet in the  $X$  direction and  $\psi$  the sweep of the wing. Hence there is obtained in place of equation (A-1)

$$\begin{aligned} \Delta p &= \kappa_X \rho_J V_J^2 \cos^2(\psi) \delta_J \quad , \\ &\simeq - J \cos^2(\psi) d^2 z / dX^2 \quad , \end{aligned} \quad (\text{A-2})$$

for a shallow jet. Here  $J = \rho_J V_J^2 \delta_J$  is the local jet momentum which is independent of  $Y$  and, for a sufficiently 'thin' jet, is invariant with  $X$ <sup>19</sup>.

Upon referring to Bernoulli's equation it is found that, for an inviscid, irrotational flow external to the jet,

$$\Delta p = \rho U_\infty \gamma_J \cos \psi \quad . \quad (\text{A-3})$$

where  $\gamma$  is the strength of the bound vortices, the axes of which are parallel to the generators of the wing, and suffix J refers to the jet. Hence equation (A-2) and (A-3) may be combined to give for the jet vortex-strength

$$\gamma_J = - (J/\rho U_\infty) \cos(\psi) d^2 z/dX^2 . \quad (A-4)$$

The condition that the normal velocity at both the wing and the jet is zero leads to the following result for the **downwash**

$$w = U_\infty dz/dx = U_\infty \cos(\psi) dz/dX, \quad z = 0, \quad X > 0 . \quad (A-5)$$

Therefore equation (A-4) may be rewritten in the form

$$\gamma_J = - (J/\rho U_\infty^2) dw/dX . \quad (A-6)$$

For an infinite sheared wing the flow may be regarded as two-dimensional in planes  $Y = \text{constant}$ . Therefore, by analogy with the linearised treatment of the two-dimensional jet-flap by **Spence**<sup>19</sup>, it is possible to write for the **downwash** on the plane  $z = 0$

$$w(X) = - \frac{1}{2\pi} \left( c_e \int_0^{\cos \psi} \frac{\gamma_W(X')}{X' - X} dX' + \int_{c_e \cos \psi}^{\infty} \frac{\gamma_J(X')}{X' - X} dX' \right) , \quad (A-7)$$

suffix W referring to the wing. Hence, upon comparing equation (A-6) and (A-7) and making use of the non-dimensional quantities

$$\xi = X/c_e \cos \psi, \quad \xi' = X'/c_e \cos \psi, \quad \bar{\gamma} = \gamma/U_\infty, \quad (A-8)$$

it is found that, with  $C'_\mu = J/\frac{1}{2}\rho U_\infty^2 c_e$  the local jet-momentum coefficient,

$$\bar{\gamma}_J = \frac{C'_\mu \sec \psi}{4\pi} \frac{d}{d\xi} \left( \int_0^1 \frac{\bar{\gamma}_W}{\xi' - \xi} d\xi' + \int_1^\infty \frac{\bar{\gamma}_J}{\xi' - \xi} d\xi' \right) . \quad (A-9)$$

This expression is an integral equation in the two unknowns  $\bar{\gamma}_W$  and  $\bar{\gamma}_J$ ; to complete the solution use is made of the boundary condition (A-5) for the

**downwash** at the wing. By combining this equation with equation (A-7) and employing equation (A-8) one obtains the result

$$\frac{dz}{dx} = \left( \int_0^1 \frac{\bar{\gamma}_W}{\xi' - \xi} d\xi' + \int_1^\infty \frac{\bar{\gamma}_J}{\xi' - \xi} d\xi' \right) \quad (A-10)$$

Equations (A-9) and (A-10) differ from the **corresponding** equations for the two-dimensional wing, of the same section and at the same incidence and **jet-momentum coefficient**, only in that  $C'_\mu$  is replaced by  $C'_\mu \sec \psi$ . Consequently, if the streamwise slope of the wing and the jet is **characterised** by the two parameters  $\alpha$ , incidence, and  $\theta$ , flap angle, it is possible to write for the bound-vortex strength of the sheared wing

$$\gamma^{(s)}(\xi, C'_\mu) = \alpha \gamma_\alpha^{(s)}(\xi, C'_\mu) + \theta \gamma_\theta^{(s)}(\xi, C'_\mu),$$

where  $\gamma_\theta^{(s)}(\xi, C'_\mu) = \gamma_\theta^{(2)}(\xi, C'_\mu \sec \psi)$ ,

$$\gamma_\alpha^{(s)}(\xi, C'_\mu) = \gamma_\alpha^{(2)}(\xi, C'_\mu \sec \psi),$$

and superscript (2) refers to the corresponding two-dimensional wing. Therefore, by referring again to Bernoulli's equation, it is found that the local lift coefficient of the sheared wing is given by

$$\begin{aligned} C_L^{(s)}(C'_\mu) &= 2 \cos \psi \int_0^\infty \left( \gamma^{(s)} / U_\infty \right) d\xi, \\ &= \cos \psi C_L^{(2)}(C'_\mu \sec \psi) \end{aligned}$$

Likewise the local, pitching-moment coefficient may be written as

$$C_m^{(s)}(C'_\mu) = \cos \psi C_m^{(2)}(C'_\mu \sec \psi),$$

the pitching-moment coefficients, like the lift coefficients, being based on the extended chord.

Appendix B

DETERMINATION OF PITCHING MOMENT

In this Appendix a description is given of the method used to evaluate the pitching moment. The method parallels the technique used to evaluate lift in section 3 and is based on a modified version of the method of Maskell and Spence. The first modification to the basic method involves an allowance for the effect of sweep. This is achieved by assuming that, for a wing of sufficiently large aspect ratio, the **spanwise** component of vorticity at any given **streamwise** section of the wing is identical to that of an infinite sheared wing of the same section, sweep and local jet-momentum coefficient. Consequently the chordwise distribution of bound vorticity predicted by the first of the interpolation methods proposed by Maskell and Spence becomes

$$\gamma(\xi) = \theta \gamma_{\theta}^{(s)}(\xi, C'_{\mu}) + (a - \alpha_{i\infty}) \gamma_{\alpha}^{(s)}(\xi, C'_{\mu}) + 2U_{\infty}(\alpha_{i\infty} - \alpha_i) \left[ (1 - \xi)/\xi \right]^{\frac{1}{2}} .$$

Here  $\gamma_{\theta}^{(s)}$ ,  $\gamma_{\alpha}^{(s)}$  = vortex distributions of the equivalent sheared wing, defined in Appendix A;

$\alpha_i$ ,  $\alpha_{i\infty}$  = induced angle of incidence at the wing, and induced angle of incidence at the vortex trace in the Trefftz plane, respectively, and

$$\xi = x/c_e .$$

Therefore the local, pitching-moment coefficient about the leading edge of the section, in the nose-up sense,  $C'_m$ , is given by

$$C'_m - C'_{m_{JR}} \equiv - 2 \int_0^1 (\gamma(\xi)/U_{\infty}) \xi d\xi = C_m^{(s)} - C_{m_{JR}}^{(s)} - \alpha_{i\infty} \left( \partial C_m^{(s)} / \partial \alpha \right) - (\alpha_{i\infty} - \alpha_i) \pi / 2, \quad \dots \dots (B-1)$$

where  $C_m^{(s)}$  is the local, pitching-moment coefficient, in the nose-up sense, about the leading edge of an infinite, sheared wing with a jet-flap (see Appendix A), suffixes JR refer to the jet reaction component of pitching moment and use has been made of the fact that  $\partial C_{m_{JR}}^{(s)} / \partial \alpha = 0$ .

According to Maskell and Spence, for the case of an elliptic distribution of circulation across the span in the Trefftz plane,

$$\alpha_{i\infty} = 2C_L / (\pi A + 2C_\mu) .$$

The assumption that the spanwise distribution of circulation in the Trefftz plane is elliptic is probably best suited to unswept wings but it will be used here for wings of small or moderate sweep on the basis that only an overall indication of the pitching moment is required. Therefore, by noting that  $C_{m_{JR}}^{(s)} = C'_{m_{JR}}$  and

$$a_1 = \frac{1}{2} \alpha_{i\infty} (1 - \sigma) ,$$

where  $\sigma$  is small, positive, equation (B-1) becomes

$$C'_m = C_m^{(s)} - 2C_L \left[ \left( \frac{\partial C_m^{(s)}}{\partial \alpha} \right) + (1 + \sigma)\pi/4 \right] / (\pi A + 2C_\mu) \quad (B-2)$$

If  $\theta$ ,  $\alpha$ ,  $C'_\mu$  and the flap chord to extended chord,  $c_f/c_e$ , are constant across the span it follows from equation (B-2) that  $C'_m$  and the local lift coefficient  $C'_L$  are independent of  $y$  the distance across the span. Therefore, in this case, the overall pitching-moment coefficient, about a point that is a distance  $x_r(y)$  downstream of the leading edge of any given wing section,

$$C_m \cong m / \frac{1}{2} \rho U_\infty^2 S \bar{c} = C'_m V + C'_{Lr} V \quad , \quad (B-3)$$

$$\text{where } V = \int_{-b/2}^{+b/2} (c_e^2(y) dy) / S \bar{c} \quad ,$$

$$V_r = \int_{-b/2}^{+b/2} (c_e(y) x_r(y) dy) / S \bar{c} \quad ,$$

$\bar{c}$  is the geometric mean chord, and

$b$  is wing span.

Therefore upon combining equations (B-2) and (B-3) it is found that

$$C_m \cong V \left[ \theta (\partial C'_m / \partial \theta) + \alpha (\partial C'_m / \partial \alpha) \right] + V_r \left[ \theta (\partial C'_L / \partial \theta) + \alpha (\partial C'_L / \partial \alpha) \right]$$

$$\text{where } C'_m = C_m^{(s)} - 2C_L \frac{\partial C_m^{(s)} / \partial \alpha + (1 + \sigma)\pi/4}{\pi A + 2C_\mu} .$$

Crude allowances for the effects of wing thickness and part-span flaps can be derived in a manner analogous to the method used in section 3 to correct the lift by writing

$$C_m = V \left\{ 1 + (2t/c_e) \sec \psi \right\} \left[ v_1 \theta (\partial C'_m / \partial \theta) + v_2 \alpha (\partial C'_m / \partial \alpha) \right] + V_r \left[ \zeta_1 \theta (\partial C'_L / \partial \theta) + \zeta_2 \alpha (\partial C'_L / \partial \alpha) \right] - (2t/c_e) \sec(\psi) V' C'_{mJR} \quad (B-4)$$

Here

$$v_1 = \frac{V'}{V}, \quad v_2 = \frac{V' (\partial C'_m / \partial \alpha) + (V - V') (\partial C'_m / \partial \alpha)_{C'_\mu=0}}{V (\partial C'_m / \partial \alpha)}$$

$$\zeta_1 = \frac{V'_r}{V_r}, \quad \zeta_2 = \frac{V'_r (\partial C'_L / \partial \alpha) + (V_r - V'_r) (\partial C'_L / \partial \alpha)_{C'_\mu=0}}{V_r (\partial C'_L / \partial \alpha)}$$

with  $V'$  and  $V'_r$  the ratios  $V$  and  $V_r$  evaluated over the reduced span appropriate to the flaps. In addition, the sectional derivatives in equation (B-4) are evaluated by using the mean sectional-momentum coefficient  $C'_\mu = C S / S'$ . The effect of thickness is allowed for by the factor  $\left\{ 1 + (2t/c_e) \sec \psi \right\}$  on the circulation component of the sectional pitching moment about the leading edge. This factor is derived by noting from classical aerofoil theory that, to first order in thickness-chord ratio, thickness does not affect the pitching moment, due to incidence, about the centre of area of an aerofoil of elliptic section. Because of the basic similarity between the flows<sup>14</sup> the same property applies to a sheared wing of elliptic section.

As in section 3, the basic method is adapted to allow for the possibility that only part of the jet is captured. In addition, the momentum coefficient  $C'_\mu$  is replaced by  $C'_{\mu c}$  and the effective flap angle  $\theta$  is assumed equal to the overall flap angle.

As well, consideration is given to allowance for non-linearities and boundary-layer effects associated with flap deflection. The change in the local pitching moment arising from these effects is conveniently separated into changes in (a) the circulation component, and (b) the jet-reaction component. The alteration to the first component may be considered to result from two effects, namely:

- (i) an alteration in circulation lift, the centre of circulation lift being fixed in the streamwise sense;
- (ii) a change in the streamwise position of the centre of circulation lift at constant circulation lift.

The first of these effects has been discussed in section 3 and can be included by multiplying the linear approximation for the increment in the circulation component of the local pitching moment due to flap deflection,  $(AC'_{m_\theta})_\ell^{(\Gamma)}$ , by the factor  $G(C'_{\mu_c})H(\theta_F, \alpha)$ . An empirical allowance is made for the second effect by noting that the streamwise position of the centre of lift of a **two-dimensional**, flat plate downstream of the leading edge varies as  $\cos \alpha$  with incidence. This suggests the derivation of a factor

$$K = \cos \alpha - (\cos \theta_F - \cos \alpha) \left[ \left( \frac{\Delta C_{m_\theta}^{(2)}}{\Delta C_{m_\theta}^{(2)}} \right)_f / \Delta C_{m_\theta}^{(2)} \right]_{C'_\mu=0},$$

$$\approx 1 - (\cos \theta_F - 1) \left[ \left( \frac{\Delta C_{m_\theta}^{(2)}}{\Delta C_{m_\theta}^{(2)}} \right)_f / \Delta C_{m_\theta}^{(2)} \right]_{C'_\mu=0},$$

which is applied to the circulation component  $(AC'_{m_\theta})_\ell^{(\Gamma)}$ , the suffix f

referring to the contribution of the flap. Thus, with the linear lift increments  $\theta \partial C'_L / \partial \theta$  and  $\alpha \partial C'_L / \partial \alpha$  of equation (B-4) replaced by their non-linear equivalents,  $\Delta C'_{L_\theta}$  and  $AC'_\alpha$  the final expression for the pitching moment becomes

$$C_m = K G(C'_{\mu_c}) H(\theta_F, \alpha) v \left( \Delta C'_{m_\theta} \right)_\ell^{(\Gamma)} + v \left( \Delta C'_{m_\alpha} \right)_\ell^{(\Gamma)} + v_r \left[ \zeta_1 \Delta C'_{L_\theta} + \zeta_2 \Delta C'_{L_\alpha} \right] + C_{m_{JR}}, \quad (B-5)$$

where the jet-reaction component about the leading edge of the wing at the **spanwise** station of the nacelle axis  $C_{m_{JR}}$  comprises two contributions. The first,  $-C_{\mu_c} \sin(\theta_c) (c_e - c_f) / \bar{c}$ , is due to the captured part of the jet and the second, which is attributable to the uncaptured area of the jet is given by:

$$AC_{m_f} = (M_J - M_c) z_r / \frac{1}{2} \rho U_\infty^2 S \bar{c} ,$$

$z_r$  being the minimum distance of the centre of the cross-sectional area of the uncaptured part of the jet below the reference axis.

Finally, for the sake of consistency with the method in section 3, the parameter  $\sigma$  was placed equal to zero in the calculations leading to the theoretical curves of Figs. 16 and 17.

Table 1

Flap configuration	Flap		Tab		Symbol
	$g_1/c$	$l_1/c$	$g_2/c$	$l_2/c$	
40/0(u)	0.015	0.020	0	0.015	X
40/10(u)	0.015	0.020	0	0.015	A
30/20(u)	0.015	0.020	0	0.015	⊖
40/30(s)	0.015	0.020	0.009	-0.002	0

NB:  $g$  = gap

$l$  = overlap

suffixes 1 and 2 refer respectively to flap and tab

SYMBOLS

A	aspect ratio of wing with high-lift devices retracted	
b	wing span	
$C_A$	longitudinal force coefficient	} referred to planform area S
$C_{D_0}$	boundary-layer drag coefficient	
$C_{D_M}$	intake-momentum drag coefficient	
$C_L$	lift coefficient	
$C_{T_G}$	nacelle gross-thrust coefficient	
$C_m$	pitching-moment coefficient, = $m/\frac{1}{2}\rho U_\infty^2 S \bar{c}$	
$C_L^{(s)}$	sectional lift coefficient of sheared wing	} referred to chord $c_e$
$C_m^{(s)}$	sectional pitching-moment coefficient of sheared wing	
$C_\mu$	overall jet-momentum coefficient	
$C'_\mu$	sectional jet-momentum coefficient	
$\bar{c}$	geometric mean chord of wing with high-lift devices retracted	
$c_e$	extended chord of wing	
$D_J$	diameter of jet	
F	aspect-ratio factor defined in equation (15)	
g	flap or tab gap	
$G(C'_\mu)$	factor allowing for effect of flap boundary layer on incremental circulation due to flap deflection	
$H(\theta_F, \alpha)$	factor allowing for non-linearities in relationship between incremental circulation lift, due to flap deflection, incidence and flap deflection	
J	local jet momentum	
K	factor allowing for streamwise movement of centre of lift due to non-linear effects of incidence and flap deflection	
ℓ	flap or tab overlap	
M	momentum flux	
m	pitching moment	
s	= $S_e/S$	
$S_e, S$	planform area of wing with and without high-lift devices deployed, respectively	

SYMBOLS (continued)

$t$	maximum thickness of wing
$U_\infty$	main-stream speed
$V$	$= \int_{-b/2}^{b/2} (c_e^2(y) dy) / S\bar{c}$
$V_r$	$= \int_{-b/2}^{b/2} (c_e(y) x_r(y) dy) / S\bar{c}$
$V', V'_r$	$V$ and $V_r$ evaluated over reduced span appropriate to the flaps
$V_J$	jet velocity in free-stream direction
$V_1, V_2$	velocities in jet along lines of curvature of jet sheet
$W$	<b>downwash</b> velocity
$x, y, z$ $X, Y, Z$	} left-handed Cartesian coordinate systems defined in Fig.18
$x_r(y)$	
$\alpha$	angle of incidence
$\alpha_f$	induced angle of incidence at wing
$\alpha_{i\infty}$	induced angle of incidence at vortex trace in Trefftz plane
$\gamma$	strength of bound vortices, the axes of which are parallel to generators of sheared wing
$\bar{\gamma}$	$= \gamma / U_\infty$
$A$	incremental part of
$\delta_J$	jet thickness
$\zeta_1, \zeta_2$	<b>terms</b> defined in equations (B-5)
$\eta$	thrust-recovery factor
$\theta$	effective flap angle
$\theta_F$	overall flap angle, $= \theta_{F1} + \theta_{F2}$
$\theta_{F1}$	flap deflection
$\theta_{F2}$	tab deflection relative to flap

SYMBOLS (concluded)

$\theta_{Fu}$	angle between line tangential to upper boundary of flap at flap trailing edge and reference axis in chordwise plane
$\theta_c$	angle between momentum vector of captured flow and reference axis in chordwise plane
$\theta_J$	jet deflection angle
$\kappa$	correlation parameter defined in equation (6)
$\kappa^*$	value of $\kappa$ when jet is fully captured
$\kappa_1, \kappa_2$	principal curvatures of jet sheet
$\kappa_X$	curvature of jet sheet in X direction
$\lambda$	$= 2z_T/D_J$
$\mu_1$	$= S'/S_e$
$\mu_2$	$= \left[ s' \left( \frac{\partial C_L^{(s)}}{\partial \alpha} \right) + (S_e - S') \left( \frac{\partial C_L^{(s)}}{\partial \alpha} \right)_{C'_\mu=0} \right] / S_e \left( \frac{\partial C_L^{(s)}}{\partial \alpha} \right)$
$\nu_1, \nu_2$	terms defined in equations (B-5)
$\xi$	$= X/c_e \cos \psi = x/c_e$
$\rho$	density of main flow
$\sigma$	small positive number in equation (15)
$\phi_e$	jet pitch angle
$\psi$	sweep angle

Suffixes

c	refers to captured part of jet
f	refers to flap
J	refers to jet as a whole
l	denotes value given by linearised theory
n	refers to position of 'hot-jet' exit of nacelle in chordwise plane containing nacelle axis
(u), (s)	refer respectively to an unslotted or slotted tab
$\alpha$	due to angle of incidence
( $\Gamma$ )	denotes circulation component
$\theta$	due to flap angle

REFERENCES

<u>No.</u>	<u>Author</u>	<u>Title, etc.</u>
1	M.R. Mendenhall M.F.E. Dillenius S.B. Spangler	Calculation of aerodynamic characteristics of STOL aircraft with externally-blown jet-augmented flaps. AIAA Paper 72-63 (1972)
2	Ely S. Levinsky Joseph C. Ramsey	Methodology for estimating STOL aircraft high-lift system characteristics. AIAA Paper 72-779 (1972)
3	D.H. Perry	A review of some published data on the external-flow jet-augmented flap. (Appendix by D.N. Foster) ARC CP 1194 (1970)
4	M.L. Lopez C.C. Shen	Recent developments in jet flap theory and its application to STOL aerodynamic analysis. AIAA Paper 71-578 (1971)
5	P.R. Ashill S.F. Mansfield	Note on some exploratory tests on a swept wing with an external-flow jet-augmented flap, RAE Technical Report 72192 (ARC 34476) (1973)
6	P. Kuehl D. Welt	Externally-blown flaps, aerodynamic feasibility study of a STOL transporter. Aircraft Engineering November 1971
7	L.P. Parlett M.P. Fink D.C. Freeman	Wind-tunnel investigation of a large jet transport model equipped with an external-flow jet flap. NASA TN D-4928 (1968)
8	D.C. Freeman L.P. Parlett R.L. Henderson	Wind-tunnel investigation of a jet transport configuration with an external-flow jet flap and inboard pod-mounted engines. NASA TN D-7004 (1970)
9	D. Küchemann J. Weber	<i>Aerodynamics of propulsion.</i> McGraw-Hill, London (1953)
10	L.P. Parlett J.P. Shivers	Wind-tunnel investigation of an STOL aircraft configuration equipped with an external-flow jet flap. NASA TN D-5364 (1969)

REFERENCES (concluded)

<u>No.</u>	<u>Author</u>	<u>Title, etc.</u>
11	E.W. Graham P.A. Lagerstrom R.M. <b>Licher</b> B.J. Beane	A preliminary theoretical investigation of the effects of propellor slipstream on wing lift. Douglas Rep. SM 14991 (1953)
12	J. Williams S.F.J. Butler M.N. Wood	The aerodynamics of jet flaps. ARC R&M 3304 (1961)
13	E.C. Maskell D.A. Spence	A theory of the jet flap in three dimensions. <b>Proc. Roy. Soc., A, Vol.251, pp.407-425 (1959)</b>
14	B. Thwaites (Ed)	<i>Incompressible aerodynamics.</i> Clarendon Press, Oxford, p.327 (1960)
15	D.N. Foster P.R. <b>Ashill</b> B.R. Williams	The nature, development and effect of the viscous flow around an aerofoil with high-lift devices. ARC CP 1258 (1972)
16	J.A. Hay W.J. Eggington	An exact theory of a thin aerofoil with large flap deflection. <b>J.R.Ae.S., Vol.60, pp.653-757 (1956)</b>
17	C.C. Smith	Effect of engine position and high-lift devices on aerodynamic characteristics of an external-flow jet-flap STOL model. NASA TN D-6222 (1971)
18	M.N. Wood	The use of injector units for engine simulation on wind tunnel models at high speeds. RAE Technical Report 71215 (ARC 33505) <b>(1971)</b>
19	D.A. Spence	The lift coefficient of a thin, jet-flapped wing. <b>Proc. Roy. Soc. A, 238, <u>46</u> (1956)</b>



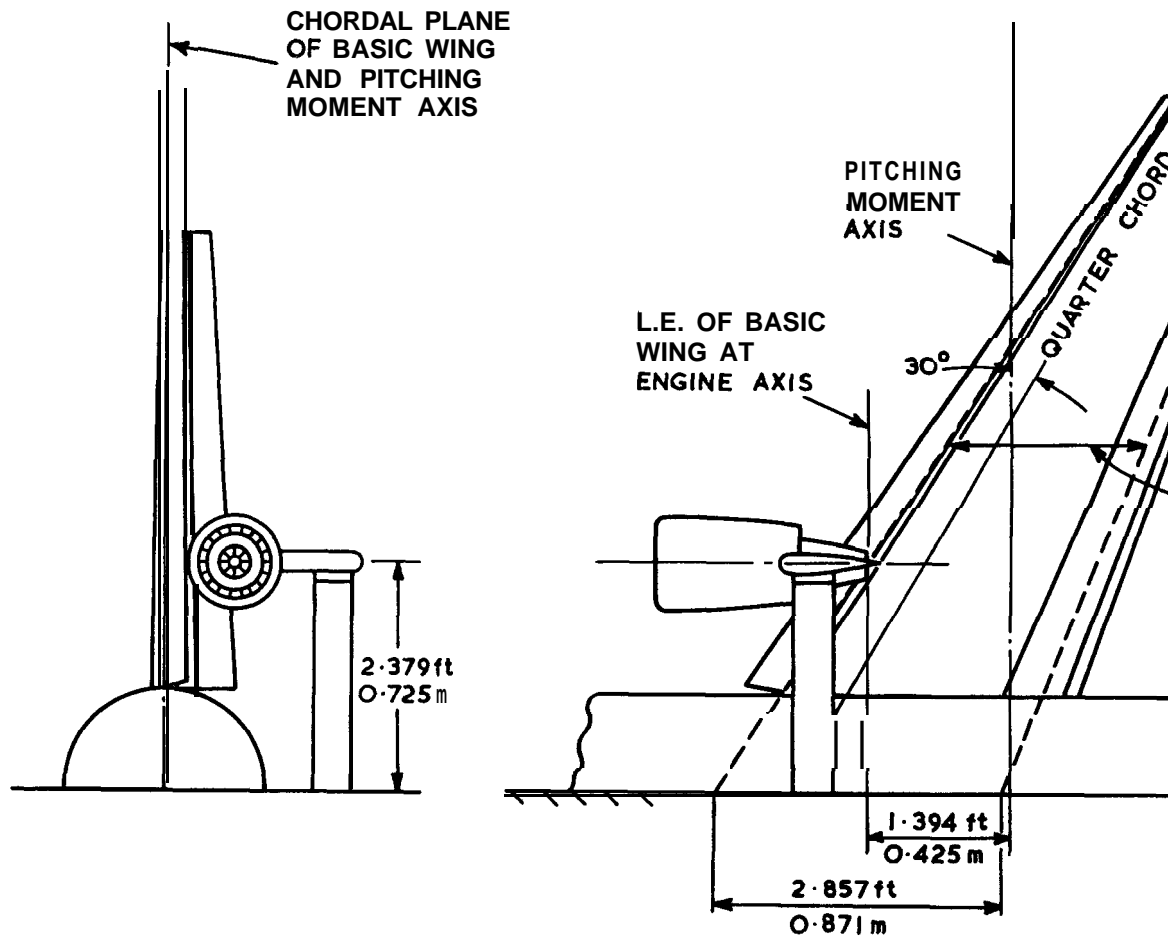


FIG. 2 GEOMETRY OF RAE, EXTERNAL - FLOW, JET-FLAP





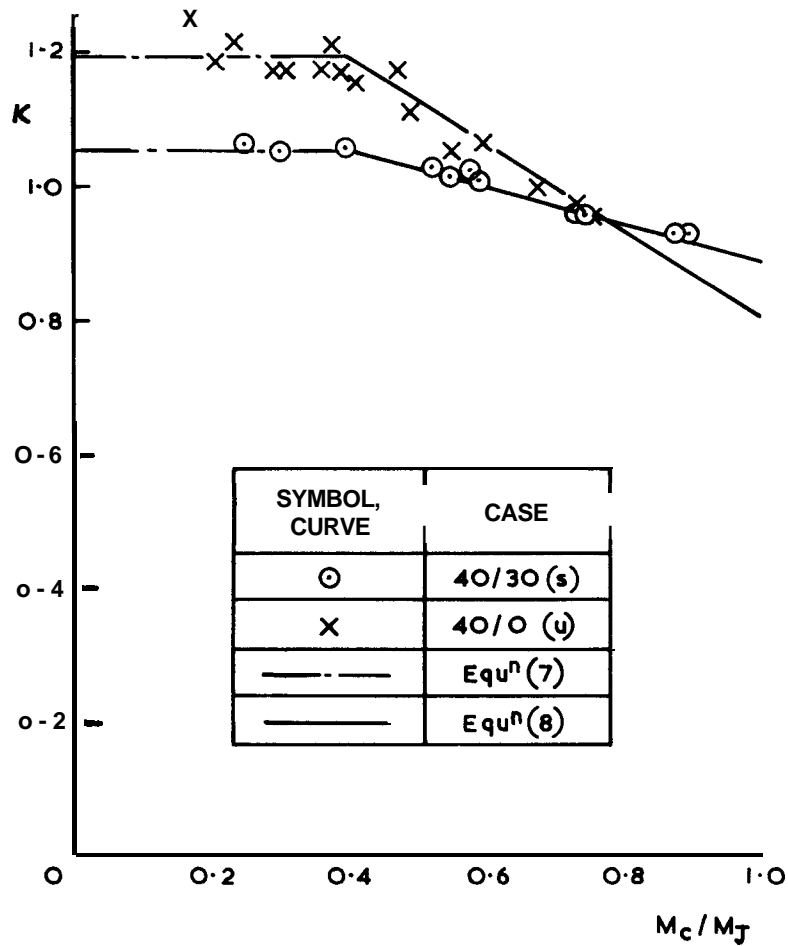


FIG.6 TURNING PARAMETER  $K$  PLOTTED AGAINST RATIO OF MOMENTUM FLUX CAPTURED BY FLAP TO OVERALL JET MOMENTUM FLUX

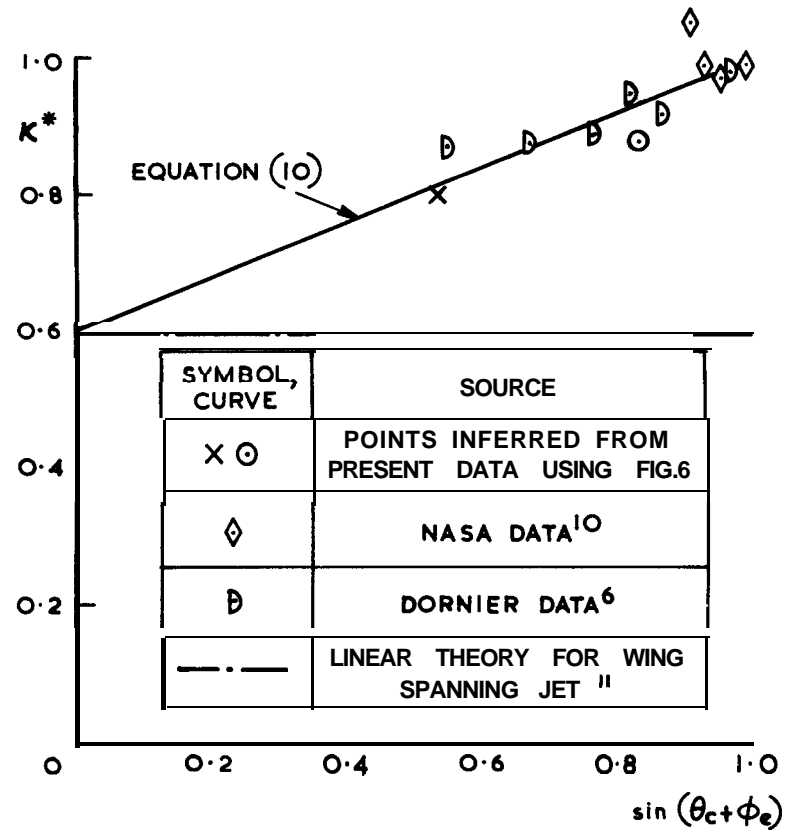
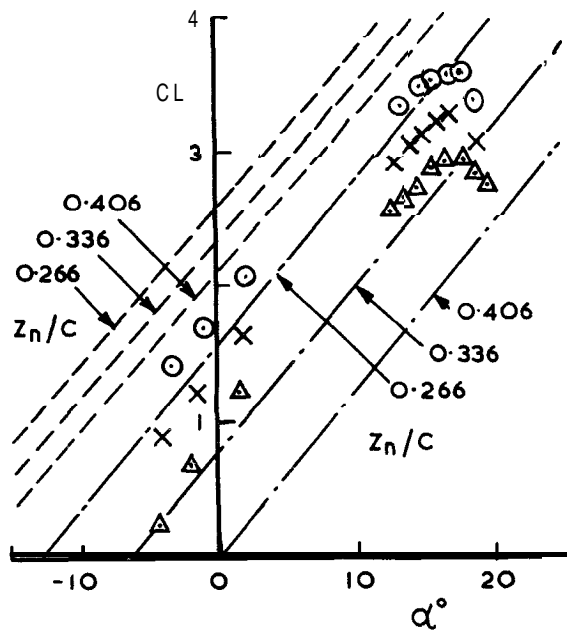
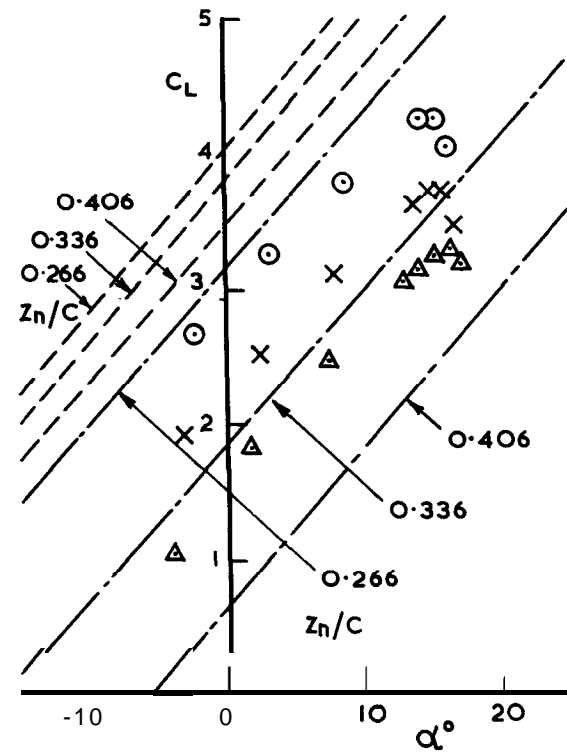


FIG.7 TURNING PARAMETER ASSOCIATED WITH FULLY -CAPTURED JET,  $K^*$ , CORRELATED AGAINST TOTAL ANGLE TURNED BY JET



a 40/0 (u)

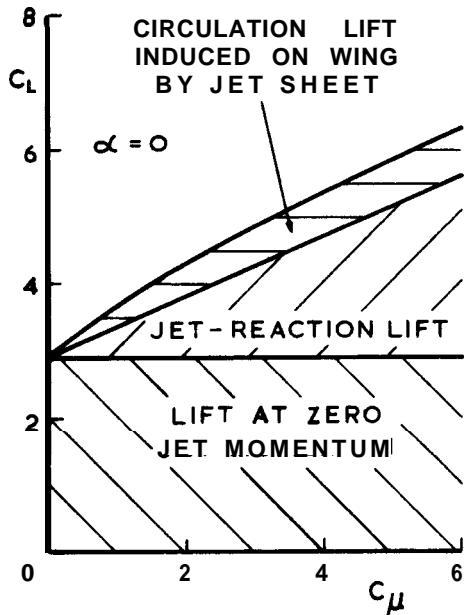
SYMBOL, CURVE	CASE	
	○	$z_n/c = 0.266$
X	$z_n/c = 0.336$	
△	$z_n/c = 0.406$	
- - -	Eq (16) $\theta = \theta_T$ PERRY'S APPROACH	
-----	PRESENT ALTERNATIVE APPROACH	



b 40/30 (s)

FIG.8a&b COMPARISON BETWEEN TEST DATA FROM RAE  
MODEL AND TWO ESTIMATION METHODS

$$(C_{TG} = 0.82, x_n/c = 0.132, \phi_e = 4.4^\circ)$$



CONFIGURATION  
 $A = 7, \psi = 0, s = 1.24$   
 $\mu_i = 1, \theta_F = 40^\circ, \lambda = 0.25$

FIG. 9 THEORETICAL BREAKDOWN OF LIFT FOR TYPICAL CONFIGURATION

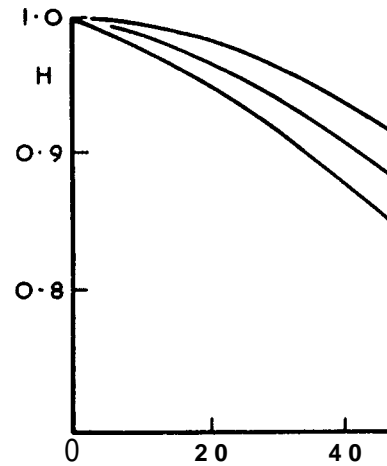


FIG.10 NON- LINEAR PARAMETER H, I THEORY OF HAY / AS A FUNCTION FLAP ANGLE A  $C_f/C_e$

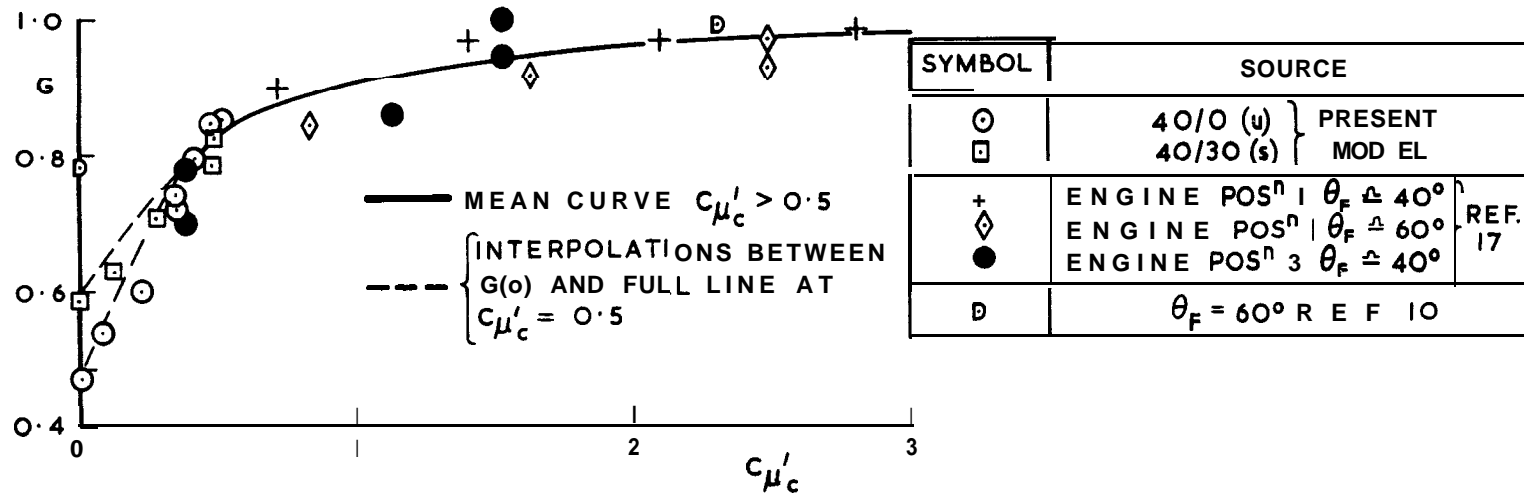
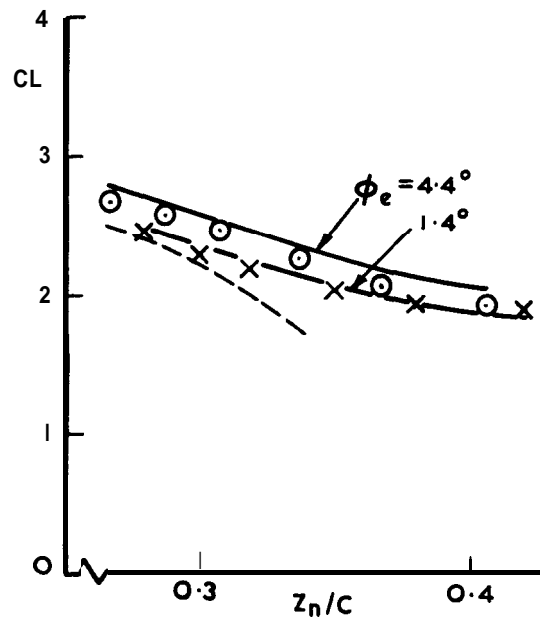
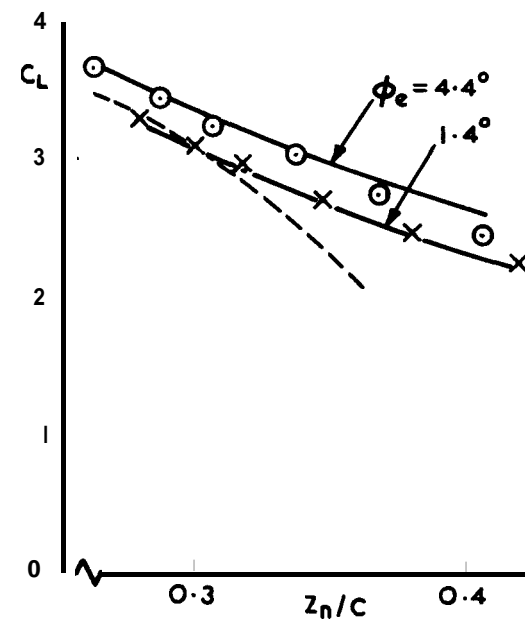


FIG. II CORRELATION BETWEEN CIRCULATION- LIFT PARAMETER  $G$  AND THE SECTIONAL- MOMENTUM COEFFICIENT OF THE CAPTURED FLOW,  $C_{\mu'_c}$



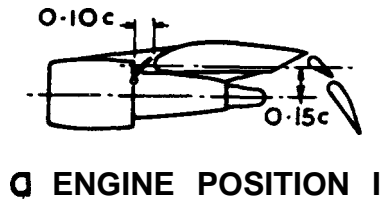
a 40/0(u)

SYMBOL, CURVE	CASE
○ X	TEST DATA
—	PRESENT METHOD Equ <sup>n</sup> (19)
- - -	PERRY'S METHOD $\theta = \theta_J, \phi_e = 4.4^\circ$



b 40/30(s)

**FIG.12a & b** EFFECT OF NACELLE HEIGHT ON LIFT: COMPARISON BETWEEN RESULTS FROM PRESENT WIND-TUNNEL TESTS ( $C_{TG} = 0.82, x_n/c = 0.132, \alpha = 7^\circ$ ) AND ESTIMATION METHODS



SYMBOL, CURVE	CASE
□ ▲	NASA TEST 17
—	PRESENT METHOD Equ <sup>n</sup> (19)
---	PERRY'S METHOD $\theta = \theta_J$

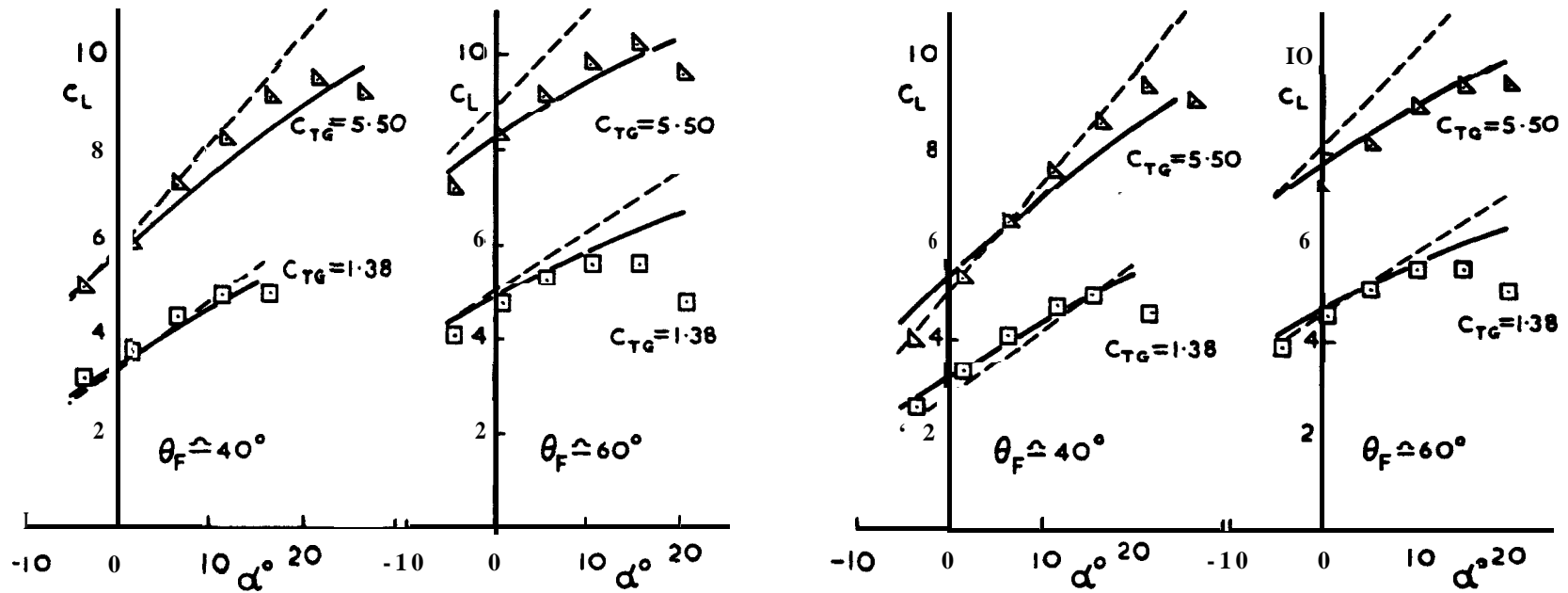
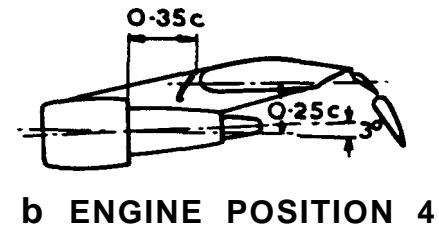


FIG.13 a&b COMPARISON BETWEEN WIND-TUNNEL TEST-DATA OF REF. 17  
AND TWO ESTIMATION METHODS

SYMBOL, CURVE	CASE
○	TEST DATA
X	
△	
—	Eqn <sup>n</sup> (22)

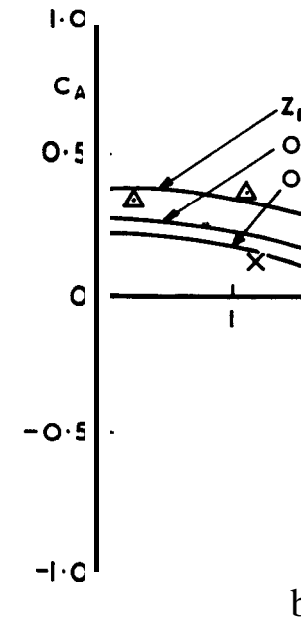
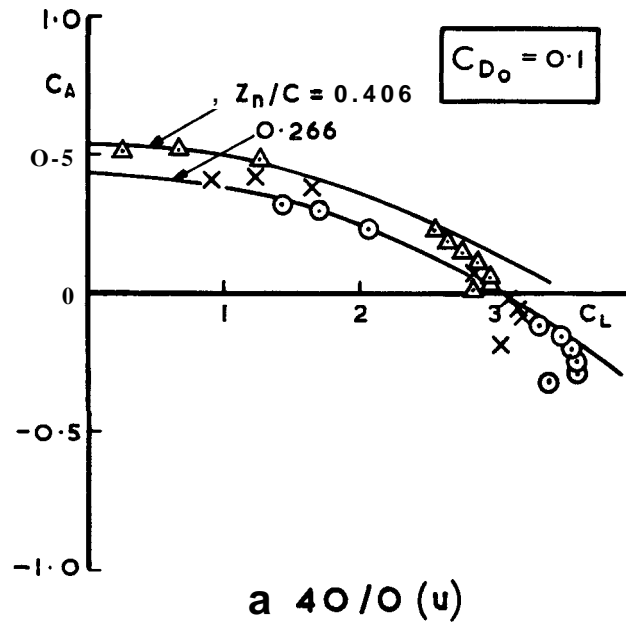
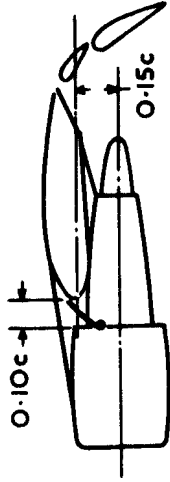
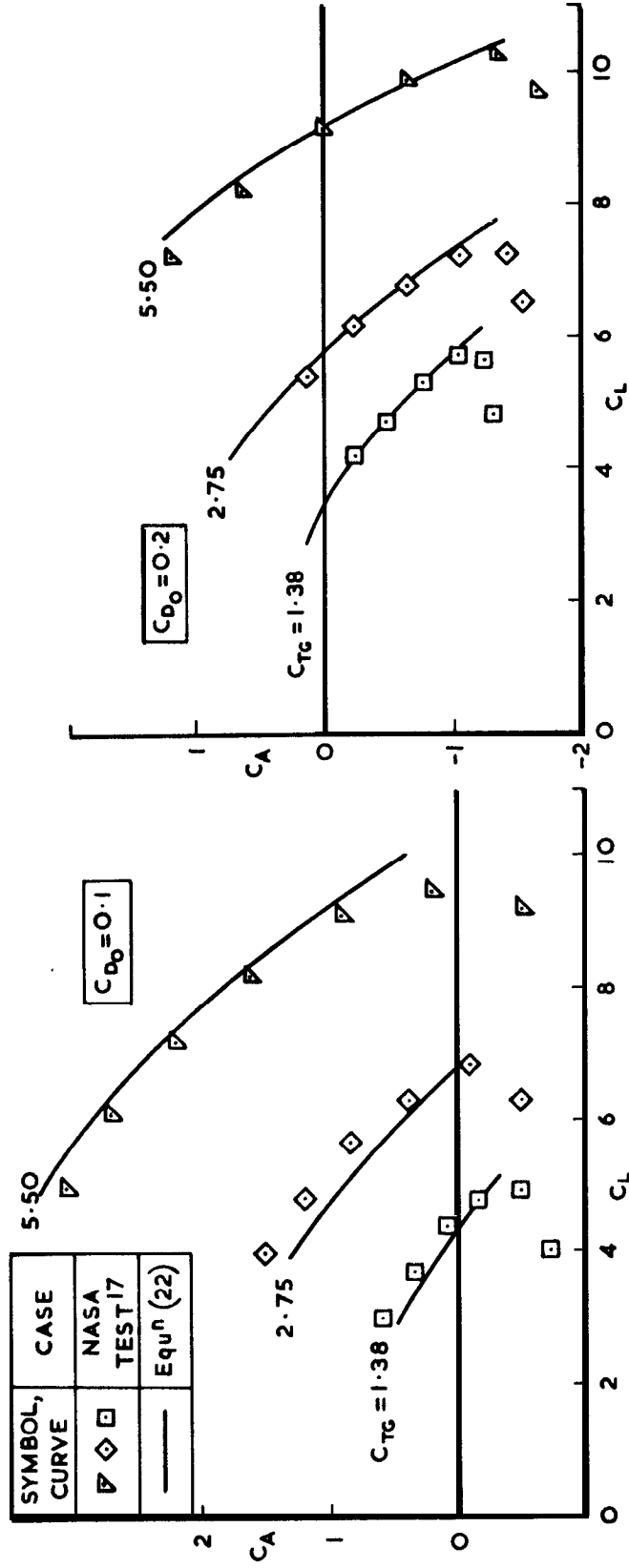


FIG. 14 a & b EFFECT OF NACELLE HEIGHT ON RELATION LONGITUDINAL FORCE AND LIFT: COMPARISON BETWEEN PRESENT TESTS ( $C_{T_0} = 0.82$ ,  $Z_n/C = 0.132$ ,  $\phi_e = 4.4^\circ$ ) A



ENGINE POSITION I



a  $\theta_F \triangleq 40^\circ$

b  $\theta_F \triangleq 60^\circ$

FIG. 15 a & b LONGITUDINAL FORCE PLOTTED AGAINST LIFT : COMPARISON BETWEEN WIND-TUNNEL RESULTS OF REF. 17 AND THRUST-DEFLECTOR THEORY

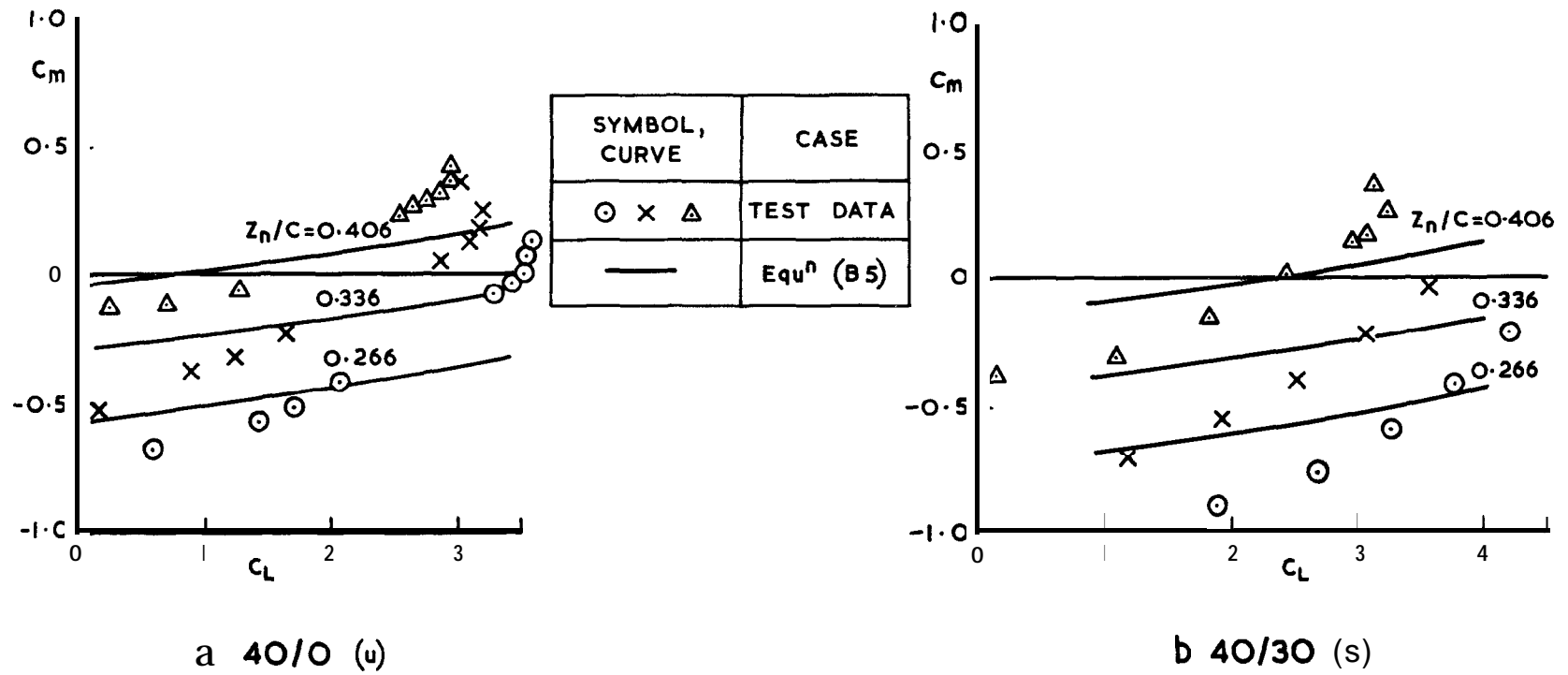


FIG. 16a & b EFFECT OF NACELLE HEIGHT ON PITCHING MOMENT  $\sim$  LIFT CURVES : COMPARISON BETWEEN RESULTS OF PRESENT TESTS ( $C_{TG} = 0.82$ ,  $\alpha_n/c = 0.132$ ,  $\phi_e = 4.4^\circ$ ) AND METHOD OF APPENDIX B

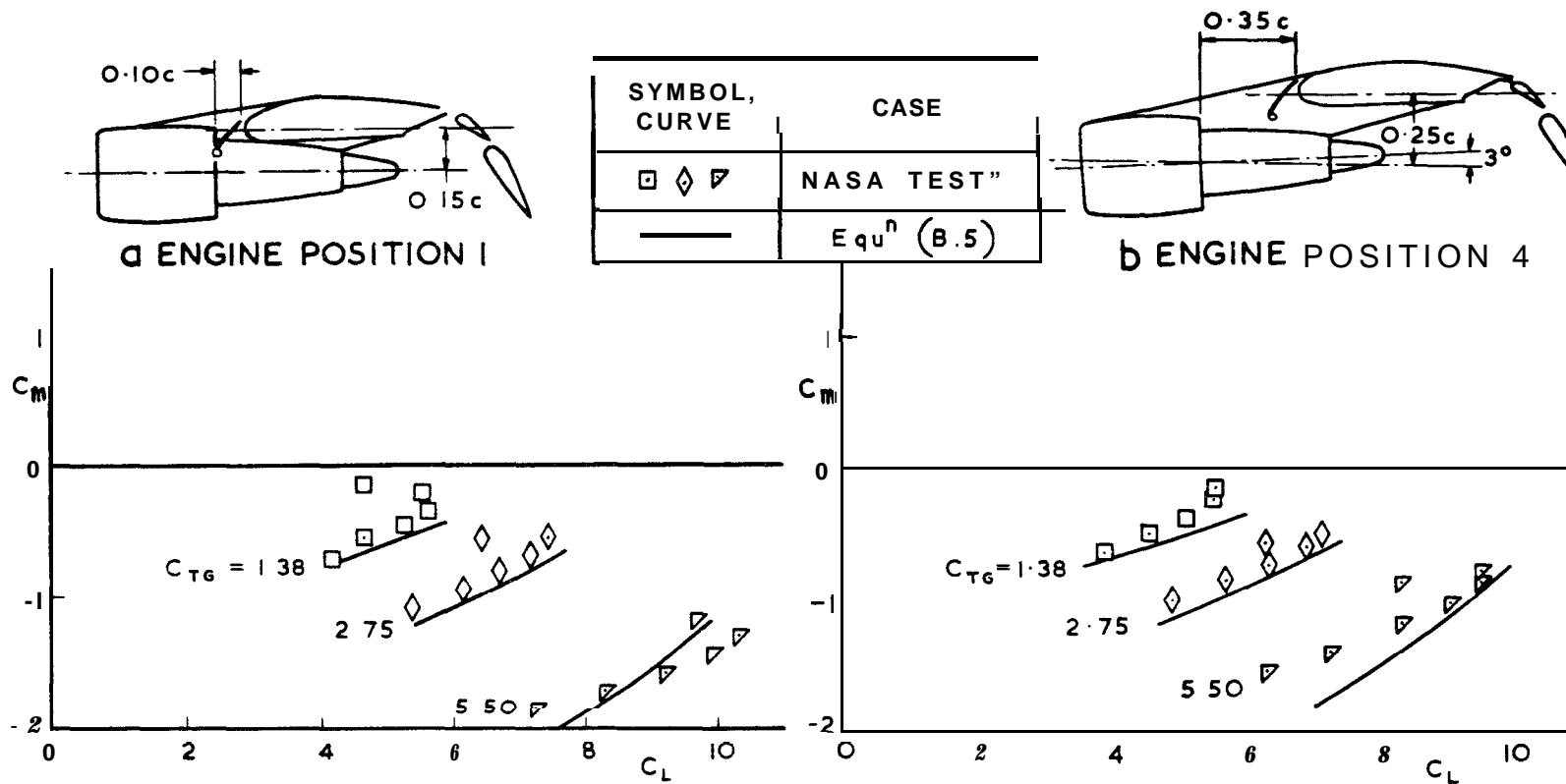


FIG. 17 a & b EFFECT OF THRUST ON PITCHING MOMENT  $\sim$  LIFT CURVES: COMPARISON BETWEEN WIND-TUNNEL RESULTS OF REF. 17 AND METHOD OF APPENDIX B  $\theta_F \approx 60^\circ$

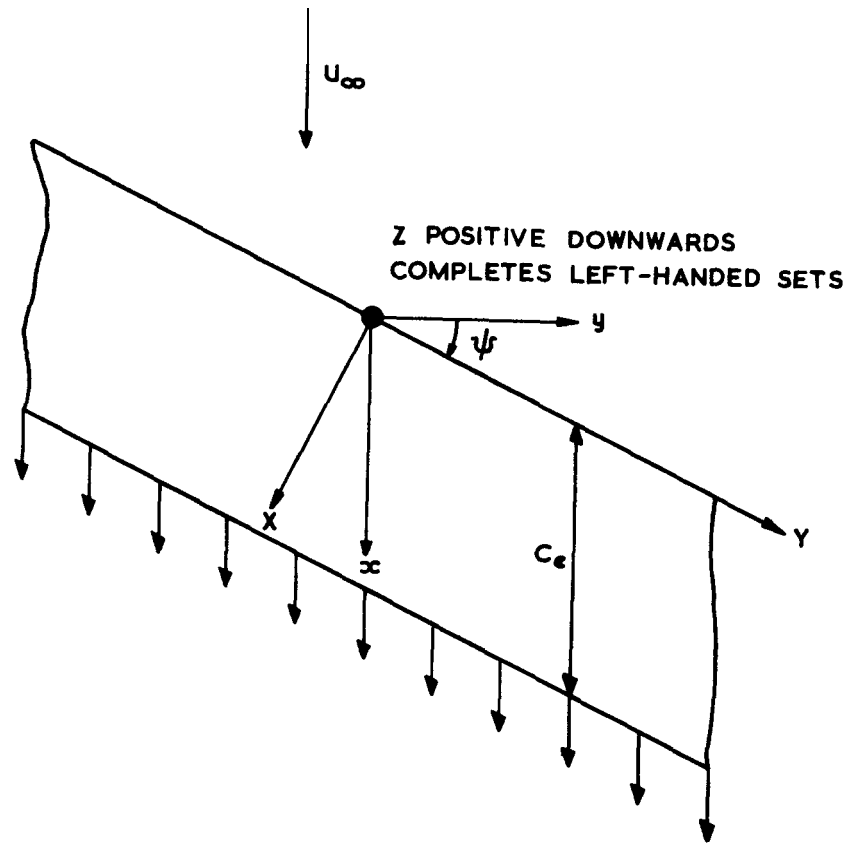


FIG.18 COORDINATE SYSTEMS FOR SHEARED WING WITH JET FLAP

C.P. No. 1319

 *Crown copyright*

1975

Published by  
HER MAJESTY'S STATIONERY OFFICE

***Government Bookshops***

49 High Holborn, London **WC1V 6HB**  
**13a** Castle Street, Edinburgh **EH2 3AR**  
41 The Hayes, Cardiff **CF1 1JW**  
Brazennose Street, Manchester **M60 8AS**  
Southey House, Wine Street, Bristol **BS1 2BQ**  
258 Broad Street, Birmingham **B1 2HE**  
80 Chichester Street, Belfast **BT1 4JY**

*Government Publications are also available  
through booksellers*

C.P. No. 1319

ISBN 011 470929 7